

## A three-dimensional model of the hip joint

J. Manuceau (*Pointe-à-Pitre, Guadeloupe*)

Université des Antilles et de la Guyane, U.F.R. Sciences Exactes et Naturelles, Département de Mathématiques, B.P. 592,  
97167 Pointe-à-Pitre, Guadeloupe.

### SUMMARY

The main aim of this work was to build a theoretical three-dimensional model of the hip. It was developed as a generalization from the model by Pauwels, which is two-dimensional.

The material used was general mechanics, to which we have added an axiom which has enabled us to calculate the distribution of surface pressures. In this way, using this theory, one can obtain the experimental results of photo-elasticity.

This model allows an analysis to be made of

the forces acting on the hip and their biomechanical role during walking. This leads to a better understanding of biomechanical failure as the cause of pathological lesions and a better choice of surgical correction.

The calculation of the distribution of surface pressures enables us to understand the position of acetabular subchondral thickening. Our results contradict those of Bombelli (1).

The first experimental model of gait was constructed by Braune and Fischer (2, 3). Their results made it possible for Pauwels (11) to construct the first theoretical model of the hip.

Since then, there has been an extraordinary development of experimental models of the hip [Macquet and Anh (9), Paul (10), Kummer (7)]. Being based, frequently, on Braune and Fischer's work, they have recently received support from computerization [Li (8)]. However, it must not be forgotten that these are descriptive models since they only have access to the resultants of forces. Their value is in making an approximation to reality.

The specific role of theoretical models is a study of their biomechanical action in relation to each force, which allows us to understand their physiology and pathology. These are explanatory models. The surgical procedure to be made is a natural one since one can calculate in advance the biomechanical consequences of it.

In this duality, theoretical models and experimental models are not antagonistic but complementary to each other. The theoretical model has to discover results from the experimental model and to provide new ones. Conversely, experimental models can demonstrate the limitations of theoretical models: this is what we have done at the conclusion of our work.

### 1. SURFACE PRESSURES

The textbook by Buhot and Thuiller (4) provides an excellent introduction to static mechanics.

#### 1.1. Flat surfaces

*1.1.1.* Let us suppose that a solid has a contact surface  $S$  with a plane  $P$  (*fig. 1*). Let  $I$  be the centre of  $S$  and  $R$ , the resultant of the forces applied to the solid. Suppose that the direction of  $R$  is at right angles to  $S$  and passes through  $I$ .

Reprints: J. MANUCEAU, address as above.

The French and English title of this paper is indexed in the main international data banks under the head « Revue de Chirurgie Orthopédique » (*Rev Chir Orthop*, 1991, 77, 293-300).

Meary Code Number : 4174.0

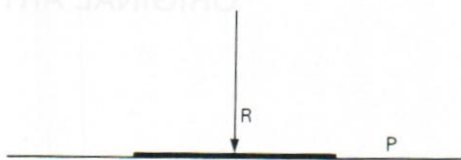


Figure 1

The classical concept of pressure,  $p = R/S$  is a global concept. The laws of mechanics do not allow a definition or a calculation to be made of pressures  $p_i$  at each point  $i$  of the surface, called « surface pressures ». To this end, we have added the following axiom (which is in the course of experimental verification) to the laws of static mechanics :

« In the case of figure 1, if the surfaces are perfectly flat and infinitely rigid, the surface pressures  $p_i$  are equal at all points  $i$  from  $S$  to  $p$  ».

1.1.2. Now suppose that the resultant  $R$  makes and angle  $\alpha$  with the perpendicular to plane  $P'$  (fig. 2).

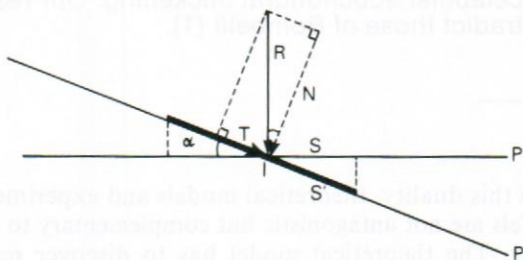


Figure 2

Let  $S'$  be the contact surface.  $R$  resolves into two forces :  $N$  orthogonal to  $P'$  and  $T$  parallel to  $P'$ .  $N$  determines the surface pressure :

$$p' = N/S'$$

$T$  is the sliding force.

1.2.3. Let us now compare the surface pressure  $p$  corresponding to the plane  $P$  with  $p'$ . We suggest that the contact surface  $S$  is the projection of  $S'$  on  $P$  and that  $P'$  and  $P$  make an angle  $\alpha$ .

We can see that :

$$S = S' \cdot \cos \alpha ;$$

$$\text{and } N = R \cdot \cos \alpha .$$

Therefore :

$$p' = N/S' = R \cos \alpha / S / \cos \alpha = \frac{R}{S} \cos^2 \alpha = p \cos^2 \alpha .$$

**1.2 Hemispherical contact surface**

1.2.1. Let us suppose that the contact surface  $S'$  is a hemisphere (fig. 3).

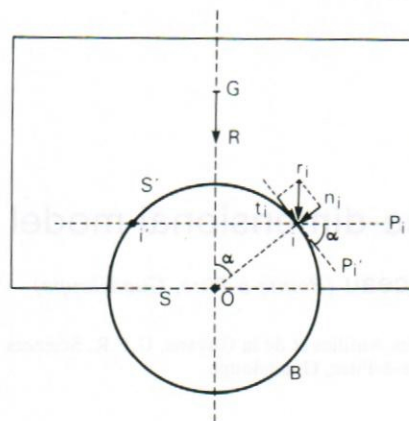


Figure 3

Let  $S$  be the surface of section of the ball  $B$  with the horizontal plane passing through its centre  $O$ .

If the support surface was  $S$ , the surface pressure  $p = F/S$  would be the same at all contact points. On the other hand, if the contact surface is  $S'$  the surface pressures are no longer constant. Let us calculate this latter at point  $i$ .

At this point there exists an infinitesimal for  $r_i$  whose component perpendicular to  $S'$  in  $n_i$  and its tangential component is  $t_i$ . Let  $s'_i$  be an infinitesimal surface  $S'$  centred on  $i$ . We can assume that  $s'_i$  is flat, contained in the plane  $P'_i$  tangential to  $S'$  at  $i$ . This latter makes an angle  $\alpha$  with the horizontal plane  $P_i$  passing through  $i$  and we note  $s_i$  which is the projection of  $s'_i$  on  $P_i$ . We find ourselves in the situation of 1.1.3. (fig. 2). Calculation shows that :

$$(1) p' = p \cos^2 \alpha .$$

We can see that the surface pressures are at their greatest at the superior pole of  $S'$  and thus equal to  $p$ , since  $\cos 0^\circ = 1$ . It decreases in proportion to the distance from the pole (fig. 4). It is nil at the equator, since  $\cos 90^\circ = 0$ .

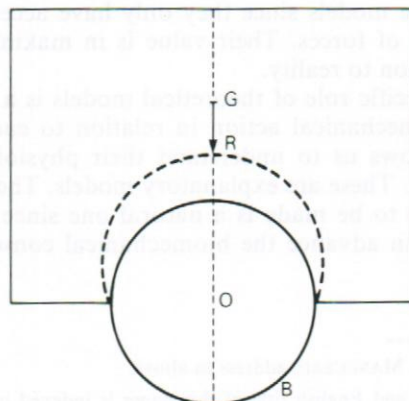


Figure 4



In conclusion, the whole of the surface pressures represented in *figure 4* (section passing through the straight line  $G0$ ), have the appearance of a crescent whose widest part is one the line  $G0$  and whose tips are at the level of the equator of the ball  $B$ . We stress the fact that the distribution of surface pressures only depends on  $R$  and not on one of its components.

1.2.2 Notes

a - The sliding force  $t_i$  (*fig. 3*) has a moment relative to the point  $0$ . If  $i'$  is the symmetrical point of  $i$  relative to the  $G0$  axis, it can be seen that the sliding force  $t'_i$  at this point has a moment relative to  $0$ , opposed to  $t_i$ . Thus there is an equilibrium.

b - Supposing that the contact surface  $S'$  is not a complete hemisphere but only a part of it, as is the case for the hip. There will be equilibrium if the surface  $S'$  has  $G0$  as its axis of symmetry. Thus the sliding forces balance in paris as we have seen above. The formulae (1) remain correct at all points of contact  $i$ , provided that we take for  $S$  the projection of  $S'$  on the equatorial plane of the ball  $B$ .

2. TWO-DIMENSIONAL MODEL OF THE HIP JOINT

We will describe here the Pauwels model and give the main results which can be drawn from it. This model describes the forces exerted in the frontal plane. It allows us to understand the model in three dimensions of which it is an extension. We can then explain our differences from Bombelli's (1) theory.

2.1. Pauwels' model (11)

Pauwels had the great merit of having conceived this model which has been the origin of extraordinary progress in the surgery of the hip in recent years.

2.1.1. Bipedal weight-bearing

In the standing position, with symmetrical weight-bearing on the two lower limbs, the centre of gravity  $S_4$  of the trunk, upper limbs and head is found, as indicated in *Figure 5*, in the mid-position of  $00'$ . The force of gravity exerted on  $S_4$  consists of a compression at each femoral head, due to a force  $R = K/2$ .  $R$  has a normal value equal to about one third of the body weight.

2.1.2. Monopedal weight-bearing

In monopedal weight-bearing, for example on the right leg, the centre of gravity  $S_5$  of the trunk, upper

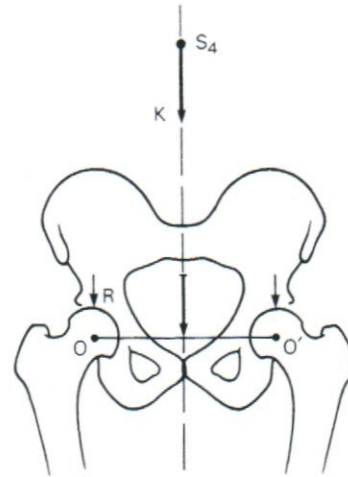


Figure 5

limbs, head and left lower limb is projected on  $00'$  at  $C$  (*figure 6*).

$0'C$  is obviously smaller than  $OC$ . The force of gravity  $K$  which is applied at  $S_5$  has a moment in relation to the centre of rotation  $0$ , equal to  $\|K\| OC$ . To balance this moment, two groups of abductor muscles play a part :

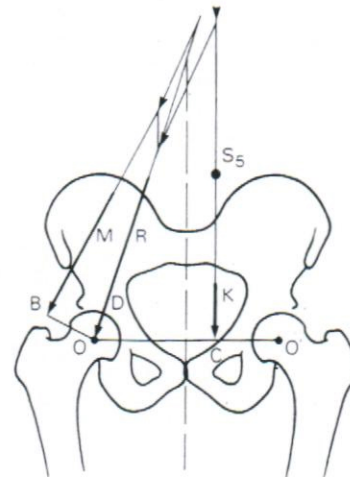


Figure 6

The pelvi-trochanteric group (gluteus medius, gluteus minimus and piriformis) and the pelvi-crural group (tensor fasciae latae, rectus femoris and sartorius). However, the principal abductor muscle is the gluteus medius.

The resultants developed by these two groups is represented by the vector  $M$  in *figure 6*. It makes an

angle of  $21^\circ$  with the vertical. The moment of this force is  $\|M\| \cdot OB$ . We know that there is equilibrium when the two moments are equal.

From this :

$$\|M\| \cdot OB = \|K\| \cdot OC$$

$$\text{and } \|M\| = \frac{OC}{OB} \cdot \|K\|.$$

The compression exerted on the femoral head is due to the resultant  $R$  of the two forces  $K$  and  $M$ . It makes an angle of  $16^\circ$  with the vertical.  $R$  passes through  $O$  and determines the distribution of surface pressures between the acetabulum and the head. It has been seen in 1.2.1. (fig. 4) that this distribution is centred on the point  $D$ . The tangential plane to the acetabulum at point  $D$  is perpendicular to  $R$ . Its angle with the horizontal is thus  $16^\circ$ .

It shows that  $TR$  has a normal value equal to about four times the body weight.

## 2.2 Bombelli's theory (1)

Bombelli starts from Pauwels model. He put forward the following hypothesis :

(H) : « the acetabular subchondral thickening is due to surface pressures exerted on the acetabulum by monopodal weight-bearing (at phase 16 of gait) ».

It should be remembered that the acetabular thickening is a subchondral sclerosis easily visible in radiographs of the pelvis. In antero-posterior pelvic views, it appears to be approximately horizontal. But we have seen in 1.2.1 (fig. 4) that the distribution of surface pressures in monopodal weight-bearing admits  $R$  as its axis of symmetry.

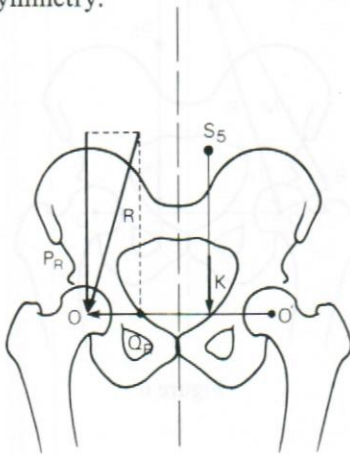


Figure 7

Consequently, if the hypothesis (H) is correct, the greatest thickness of the sclerosis should have an approximately oblique appearance, making an angle of  $16^\circ$  with the horizontal. This is rarely the case.

To explain this contradiction, Bombelli resolves  $R$  into a vertical component  $PR$  and a horizontal component  $QR$  (fig. 7).

He then asserts that the surface pressures on the acetabulum in monopodal weight-bearing are determined only by  $PR$ . This hypothesis is, at first sight, in harmony with antero-posterior radiographs of the pelvis. On the other hand, it has the irremediable defect of being in contradiction with static mechanics (cf. 1.2 and fig. 4). This same error is repeated throughout the theoretical part of Bombelli (1).

The significance of acetabular subchondral sclerosis and its position will be considered in 3.3.

## 3. THREE-DIMENSIONAL MODEL OF THE HIP JOINT

We use here the work of Braune and Fischer (2, 3) as did Pauwels for the two-dimensional model. The figures which we give are those of the authors.

### 3.1. Bipedal weight-bearing

#### 3.1.1. The biomechanical model

It is proposed that the whole upper half of the body — head, upper limbs and trunk — is a solid  $S$  with a centre of gravity  $S_4$ .  $S$  relies, through the intermediary of the acetabulae, on the right and left femoral heads with centres  $O$  and  $O'$  respectively. The femoral heads are considered as fixed (fig. 8).

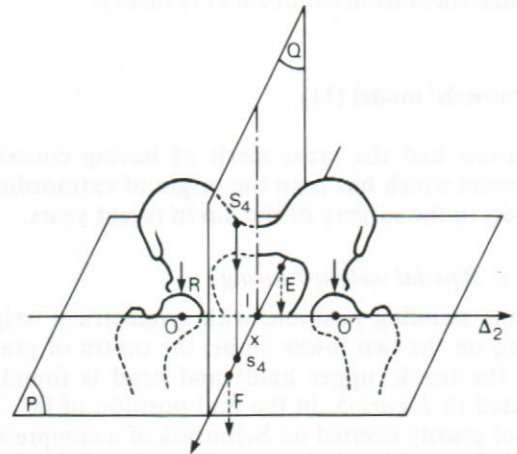


Figure 8

The forces acting on the mechanical system are :

1. The weight  $K$  of  $S$  which is applied at  $S_4$ ;
2. The resultant  $E$  of the extensor muscles (gluteus maximus and hamstrings) whose direction is considered



as vertical behind  $OO'$  and contained in the sagittal plane  $Q$  (perpendicular to  $OO'$  and passing through its centre  $I$ ). In addition it is assumed that the distance  $d_E$  of the direction of  $E$  to  $OO'$  is about 5 cm;

3. The resultant  $F$  of the flexor muscles (iliopsoas and rectus femoris) whose direction is considered as vertical and in front of  $OO'$  is contained in the sagittal plane. In addition it is assumed that the distance  $d_F$  from  $F$  to  $OO'$  is about 5 cm.

The only possible movement of  $S$  is oscillation round the axis  $\Delta_2$ . It is presumed that, in the course of this oscillation  $d_E$  and  $d_F$  do not vary in the first approximation.

It is noted that  $s_4$ , the projection of  $S_4$  on the horizontal plane  $P$ , passing through  $OO'$  and  $x$ , the distance from  $s_4$  to  $OO'$  ( $x = Is_4$ ).  $x$  is positive when  $s_4$  is in front of  $I$  and negative when it is behind it.

3.1.2. Physiology of the model

$K$  has a fixed intensity and a fixed sense. Its application point  $S_4$  oscillates round the axis  $\Delta_2$  and its direction, which is always vertical, moves in plane  $Q$ . When  $x$  is positive, then  $F = 0$  and the norm of  $E$  verifies the equation

$$\|E\| \cdot d_E = \|K\| \cdot x.$$

It is the equality of the moments  $E$  and  $K$  in relation to  $\Delta_2$ . From this

$$\|E\| = \frac{\|K\|}{d_E} \cdot x.$$

It can be seen that  $E = 0$  when  $S_4$  is in the frontal plane containing  $\Delta_2$  ( $x = 0$ ). This is the case in Pauwels' model. The greater  $\|E\|$  is, the greater  $x$  is. In that case the resultant of  $E$  and  $K$  is  $E + K$  which has a vertical direction.

To study the case when  $x$  is negative, it suffices to reverse the roles of  $E$  and  $F$ .

3.1.3. Distribution of surface pressures

For reasons of symmetry, the force which acts at each femoral head is  $R = \frac{K + E}{2}$  if  $x$  is positive; if it

is negative, it will be  $R = \frac{K + F}{2}$  and if it is nil

$$R = \frac{K}{2}.$$

$R$  thus varies in intensity, the more so as  $S$  is inclined in front or behind. The maximal value of  $R$  is obtained when  $x$  is maximal, that is to say  $x = IS_4$  ( $S_4$  is then in plane  $P$ ) which is approximately equal to 30 cm. Since  $d_E$  measures about 5 cm, it can be seen that

$$\|E_{max}\| = 6 \cdot \|K\|$$

$$\text{and } \|R_{max}\| = 3.5 \cdot \|K\|$$

The values are close to those obtained in monopodal weight-bearing. The direction of  $R$  remains fixed (ver-

tical) passing through the centre of the femoral heads. It is an axis of symmetry for surface pressures (1.4).

3.2 Monopodal weight-bearing

This model aims to describe the forces acting on the femoral head in the course of walking, where the subject is bearing weight on the right lower limb : phases 12 to 22 (fig. 9).

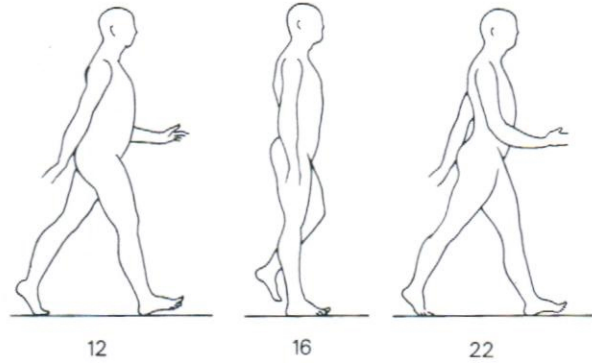


Figure 9

3.2.1. The biomechanical model

The whole upper part of the body  $S$  formed by the head, upper limbs, trunk and left lower limb has  $S_5$  for its centre of gravity. This is not a solid since the left lower limb oscillates round the axis  $OO'$ . In the course of the oscillation,  $S_5$  moves in the sagittal plane  $Q$ , intersecting  $OO'$  at  $C$ . Obviously  $OC > O'C$ ,  $S_5$  being displaced towards the left lower limb (fig. 10).

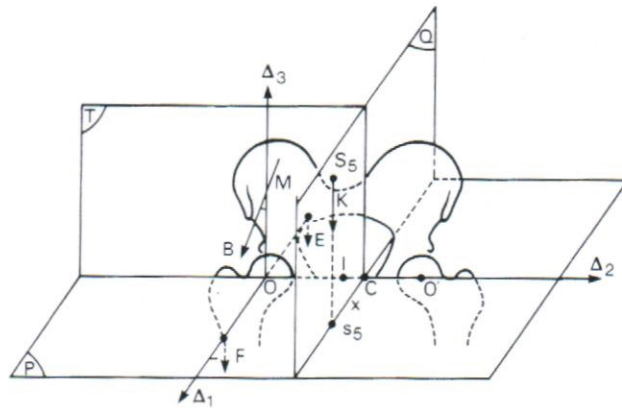


Figure 10

The forces acting on  $S$  are :

1. The body weight  $K$  applied at  $S_5$  in a vertical direction.  $K$  moves like  $S_5$  in the plane  $Q$  which is paramedian sagittal.



2. An abduction force  $M$ , situated in the frontal plane  $T$  which passes through  $O$  and  $O'$ . It makes  $S$  turn through the antero-posterior axis  $\Delta_1$  passing through  $O$ . The direction of  $M$  makes an angle of  $21^\circ$  with the vertical, according to Pauwels.

3. An extension force  $E$ , situated in the sagittal plane containing  $\Delta_1$  and  $\Delta_3$ . Its direction, contained in the plane  $(\Delta_1, \Delta_3)$  is parallel to the right lower limb. This force makes  $S$  turn round  $\Delta_2$ .

4. The flexion force  $F$  has the same characteristics as  $E$  but makes  $S$  turn in the opposite direction to  $E$ .

### 3.2.2. The physiology of the model

In order to make the exposition clearer, the calculations are given in the appendix. We will indicate the main results here.

In this model, only the static problem is of interest. The kinetic and dynamic aspects are ignored since the accelerations which affects it are very small in comparison with gravity.

As has already been mentioned,  $S$  moves round point  $O$ , the centre of the right femoral head. The force of gravity  $K$  applies to the centre of gravity  $S_5$  of  $S$ . The other forces,  $M$  of abduction,  $E$  of extension, and  $F$  of flexion only serve to balance  $K$ . Thus the moment of  $K$  in relation to  $O$  noted as  $M_0(K)$  is equal to the sum of the moments relative to  $\Delta_1$ , noted as  $M\Delta_1(K)$  and in relation to  $\Delta_2$ , noted as  $M\Delta_2(K)$ .

$M_1(K)$  makes  $S$  turn round  $\Delta_1$ . It is balanced by the moment of  $M$  in relation to  $\Delta_1$ . This problem is resolved by the Pauwels model, since  $M\Delta_1(K) = \|K\| \cdot OC$  remains constant in the course of walking.

$M\Delta_2(K)$  makes  $S$  turn round  $\Delta_2$ . It is balanced by the moment  $F$  relative to  $\Delta_2$ , when  $s_5$  is behind  $C$  (phases 12 to 15 and thus  $E = O$ ). It is balanced by that of moment  $E$  when  $s_5$  is in front of  $C$  (phases 17 to 22 and thus  $F = 0$ ). Its value is  $\|K\| \cdot x$ ; it thus varies in the course of walking. It is nil in phase 16, since  $x = 0$  and  $s_5$  is in  $C$ . It is the position of Pauwel's model, where  $M\Delta_2(K)$  does not enter into it. The moment is maximal at the extreme phases 12 and 22 where  $x = 5$  cm.

The resultant  $R$  of these four forces  $K$ ,  $M$ ,  $E$  and  $F$  varies in direction and intensity in the course of walking (fig. 11). Its direction passes through  $O$  and scans a surface which approximately resembles a portion of a cone. The resultant  $R_{16}$  at phase 16 makes an angle of  $16^\circ$  with  $\Delta_3$  (see Pauwel's model). This angle subsequently increases and reaches a value of  $18^\circ$  at the extreme phases 12 and 22.

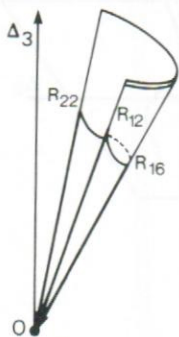


Figure 11

The intensity is minimal at phase 16 and is equal to

four times that of  $K$ . It is maximal at phases 12 and 22, equal to five times that of  $K$ .

At all times, the surface pressures admit  $R$  as axis of symmetry. In section they are crescent-shaped (fig. 4). In the course of walking they will concern the majority of the joint surface.

### 3.2.3. Comparison of the model with reality

No muscle is exclusively an abductor, flexor or extensor. This means that the resultant  $R$  is, in fact, greater than that given by the model. Consider the case of the gluteus medius. It is the principal abductor muscle. It is inserted into the greater trochanter. When anteversion of the neck is not great, the insertion point of the gluteus medius on the greater trochanter is on the axis  $\Delta_2$ . In the course of walking, this point is fixed since the right lower limb has  $\Delta_2$  for an axis of rotation. In these conditions, the gluteus medius is close to the frontal plane containing  $\Delta_2$ , and it is thus almost exclusively an abductor.

In cases where anteversion is greater, the gluteus medius is an abductor and extensor [Frain (5)]. To balance its function as an extensor, the flexors must intervene, which thus increases the resultant.

### 3.2.4. Therapeutic principles

In cases with a pathological hip, it is sometimes sufficient to diminish the norm of  $R$  to stabilize lesions and to find a new balance. This norm diminishes when:

1.  $O$  is brought closer to the centre  $I$  of  $OO'$ : pelvic osteotomies.
2. Pathological anteversion is diminished.
3. The direction of  $M$  is moved away from the centre of the femoral head  $O$ : femoral osteotomies.

## 3.3. The acetabular sclerotic line

We have already stated that the acetabular sclerotic line is the subchondral acetabular condensation visible on radiographs. We also restate the hypothesis put forward by Bombelli.

(H): « The acetabular sclerotic line is due to surface pressures which act on the acetabulum at phase 16 of walking », since the pressures are supposed to be maximal at this time.

This hypothesis seems to us to be incomplete. We have shown in 3.2 that the maximum pressures are those in phases 12 and 22 of walking. In addition, we must not take into account only maximal forces. Thus we prefer to restate the hypothesis as follows:

(H'): « The acetabular sclerotic line depends on all the surface pressures acting on the acetabulum, each one of which takes part in increasing function of its intensity and the length of time of its application.



(H') obliges us to take into account :

a) The resultants of forces in monopodal weight-bearing. We know that they are the most significant (in intensity) and are oblique.

b) The resultants of forces in bipedal weight-bearing : these are vertical. Their intensity is possibly eight to ten times less than the preceding ones but their time of application is certainly very much greater.

c) The forces developed by muscle bone : the surface forces for which they are responsible are spread over the whole of the articular surface. Their intensity is low but their time of application is much more important than all other forces.

Moreover, knowing that the distribution of surface pressures extends widely beyond the direction of the different resultant forces, we can expect the sclerosis to affect the whole of the subchondral bone. This is clearly demonstrated in radiographs :

- In antero-posterior radiographs, the condensation is often horizontal. This is due to the fact that the sclerosis is strictly subchondral. It thus stops where the bottom of the acetabulum begins and this often extends to a high level. *fig. 12* is an apposite example. It is an antero-posterior radiograph of the acetabulum whose base is very low. This is a very rare case. The sclerosis is not horizontal but occupies the whole subchondral region.



Figure 13

ures. Our model presumes that the acetabulum is an infinitely rigid solid and has a perfectly spherical shape.

To have a better approximation to reality, account should be taken of the elasticity of the pelvis and the variable shape of the acetabular cavity [Li (8), Frain (6), Teinturier *et al* (12)].

**Appendix**

$$M_0(K) = M\Delta_1(K) + M\Delta_2(K) \text{ (fig. 10), since}$$

$$M_0(K) = 0s_5 \Delta K = (OC + Cs_5) \Delta K = OC \Delta K + Cs_5 \Delta K$$

$$= M\Delta_1(K) + M\Delta_2(K).$$

$M\Delta_1(K) = \|K\|$ . OC is constant during walking and equal to the moment of M.

If  $d_E$  is the distance of O in the direction of E, in the course of phases 16 to 22, we have

$$M\Delta_2(K) = \|E\|. d_E = \|K\|. x;$$

thus 
$$\|E\| = \frac{\|K\|}{d_E}. x.$$

If we presume that  $d_E$  is approximately equal to 5 cm, since x varies from 0 to 5 cm, on sees that  $\|E\|$  varies from 0 (phase 16) to  $\|K\|$  (phase 22).

The direction E makes an angle with the vertical which varies from 0 (phase 16) and about 20° (phase 22).

For phases 12 to 16, the study of F is made in the same way.

Thus for phase 16 (Pauwels model where  $E = F = 0$ ),  $R_{16} = M + K$ , this resultant is in the frontal plane T, its direction makes an angle of 16° with the vertical  $\Delta_3$ , and its intensity  $\|R_{16}\| = 4. \|K\|$ .

For phases 16 to 22 ( $F = 0$ ),  $R = M + K + E = R_{16} + E$ .

In particular  $R_{22}$  is behind the frontal plane and makes an angle of 18° with  $\Delta_3$ ; the plane  $(\Delta_3, R_{22})$  makes an angle of 12° with the plane T. Finally

$$\|R_{22}\| = 5. \|K\|.$$

The study is identical for phases 12 to 16 ( $E = 0$ ).



Figure 12

- In oblique radiographs, the subchondral tissue which can be seen is much more extensive and part of its even vertical (*fig. 13*). The sclerosis affects the *whole* of this surface.

**CONCLUSIONS**

Whilst this model gives a satisfactory description of the forces acting on the hip, it gives, on the other hand, a less satisfactory description of the surface pres-

*Acknowledgements.* — I wish to thank J.P. Franceschi and A. Chauvin for lively and fruitful discussions which we have had together. The diagrams were by A. Giordanetto. I offer him my grateful thanks.

**References**

1. BOMBELLI R : Osteoarthritis of the hip. *Springer-Verlag*, Berlin, 1983.
2. BRAUNE W, FISCHER O : Uber den Schwerpunkt des menschlichen Körpers. *Abhandl Math. Phys. Cl. Sächs Gesellsch Wissensch*, 1889, 15, 561-589.
3. BRAUNE W, FISCHER O : Der Gang des Menschen. I. Teil. Versuche am unbelasteten und belasteten Menschen. *Abhandl Math. Phys. Cl. Sächs Gesellsch Wissensch*, 1895, 21, 153-322.
4. BUHOT G, THUILLIER P : Cours de mécanique statique. *Masson*, Paris, 1987.

5. FRAIN P : Action mécanique de l'antéversion fémorale sur la hanche. *Rev Chir Orthop*, 1981, 67, 1-9.
6. FRAIN P : Hanche normale et prothétique. *Rev Chir Orthop*, 1983, 69, 95-105.
7. KUMMER B. : Anatomie fonctionnelle et biomécanique de la hanche. *Acta Orthop Belg*, 1978, 44, 94-104.
8. LI JIA : Biomécanique de la hanche. *Thèse*, Université Clermont II, 1987.
9. MAQUET P, TUAN VU ANH : On the forces exerted on the hip during gait. *Arch Orthop Trauma Surg*, 1981, 99, 53-58.
10. PAUL JP : The biomechanics of the hip joint and its clinical relevance. *Proc R Soc Med*, 1966, 59, 943-948.
11. PAUWELS F : Biomécanique de l'appareil moteur. *Springer-Verlag*, Berlin, Heidelberg, New York, 1979.
12. TEINTURIER P, TERVER S, JARAMILLO CV, BESSE JP : La biomécanique du cotyle. SO.F.C.O.T. nov. 1983, *Rev Chir Orthop*, 1984, 70, Suppl II, 41-46.

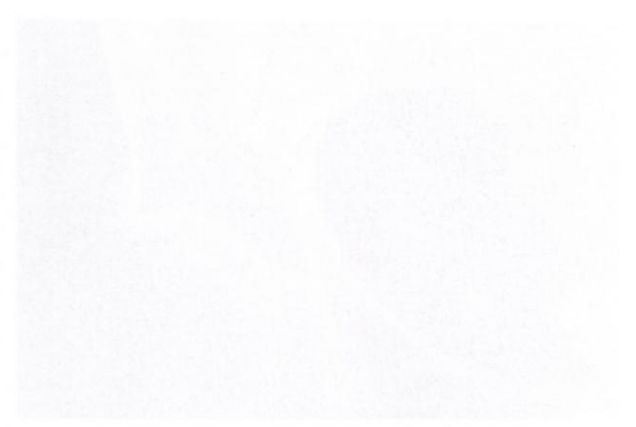


Figure 11

... in which ...

... the ...

... the ...

... the ...

... the ...